Desalination and Water Treatment
www.deswater.com
doi: 10.1080/19443994.2014.912589

54 (2015) 3400–3411
June

Taylor & Francis
Taylor & Francis Group

The adsorption of nitrate from aqueous solution onto calcined Mg/Fe hydrotalcite

Zhiquan Yang[a,b,*], Lixiang Zhang[a,b], Pan Xu[a,b], Xiaoping Zhang[a,b], Xiaojun Niu[a,b], Shaoqi Zhou[a,b]

[a]*College of Environment and Energy, South China University of Technology, Guangzhou 510006, Guangdong, China*
[b]*The Key Laboratory of Pollution Control and Ecosystem Restoration in Industry Clusters of Ministry of Education, Guangzhou 510006, Guangdong, China, Tel. +86 2013724008305; email: zqyang@scut.edu.cn*

Received 3 July 2013; Accepted 28 March 2014

ABSTRACT

A laboratory study was conducted to investigate the use of Mg/Fe hydrotalcite-like compounds for the removal of nitrate from synthetic solution. A series of calcined hydrotalcites (CHTlcs) with different chemical composition were investigated to remove nitrate. The highest nitrate percentage of adsorption (about 95%) and adsorption capacity (about 70 mg/g) were obtained by using the CHTlcs with Mg/Fe molar ratio of 3. The adsorption experiments were carried out under various equilibration conditions, such as adsorbent dose, pH, temperature, and competitive ions. It was found that 1.5 g/L Mg/Fe CHTlcs could achieve ideal adsorption efficiencies of nitrate during the nitrate adsorption process with an initial nitrate concentration of 100 mg/L at pH 8 and at temperature 30°C. Various co-existing anions interfered in the adsorption of nitrate. The inhibitory effect was in the order of phosphate > sulfate > chloride. Adsorption isotherms showed that the experimental equilibrium data was fitted better by the Langmuir isotherm model than the Freundlich. The adsorption kinetics was successfully fitted by pseudo-second-order kinetics. And the characterization of the Mg/Fe CHTlcs was also analyzed to validate adsorption process. Results showed promising utility of Mg/Fe CHTlcs that could be developed into a viable technology for nitrate removal from water.

Keywords: Mg/Fe hydrotalcite; Nitrate; Adsorption; Kinetics; Equilibrium

1. Introduction

Groundwater pollution with high nitrate concentration has become an environmental and health issue worldwide. The use of fertilizers in agriculture, chemical products, and septic tank systems are the main sources of nitrates in water [1]. Several nitrogenous compounds, including ammonia, nitrite, and nitrate have been frequently present in drinking water and various types of agricultural, domestic, and industrial wastewater. European studies recommend a maximum nitrate NO_3^- concentration of 10 mg/L, nitrite NO_2^- of 0.03 mg/L, and ammonium NH_4^+ of 0.4 mg/L in drinking water [2]. Deleterious effects of nitrate on health are well known. Nitrates and phosphates can stimulate eutrophication where pollution is caused in waterways by heavy algal growth, as they are both rate-limiting nutrients for the process [3]. The nitrite

*Corresponding author.

can cause a blue baby syndrome and it is also a precursor to the carcinogenic nitrous amine [2,4]. Water supplies contaminated by nitrate have also been linked to outbreaks of infectious disease [5].

There are a wide range of technologies to remove nitrate from water, including technologies like physical–chemical [6], biological [7–9], and so on. Biological denitrification is one of the most effective techniques to solve the nitrate problem [10]. However, possible bacterial contamination, the presence of residual organics, and the possible increase in chlorine demand in purified water limit the application of this process [11,12]. In order to overcome these shortages, physical–chemical technologies are generally considered better for drinking water treatment because of convenience, ease of operation, and simplicity of design [13]. Conventional physical–chemical techniques include ion-exchange [14,15], reverse osmosis [16], and sorption processes [17]. Further, these processes can remove/minimize different types of organic and inorganic pollutants from the water or wastewater [18,19].

Adsorption is emerging as a promising and flexible technique to remove nitrate efficiently from aqueous solution [20]. Several materials, such as activated alumina, activated carbon, bone charcoal, and so on, have been tested for the removal of nitrate by adsorption [21–23]. Although alumina is considered a potentially efficient adsorbent material, its major limitation is the reduction of about 10% in material and 40% in adsorption capacity after cyclic regenerations [24]. Activated carbon is one of the most well-known adsorbent, but its high cost restricts its comprehensive use [22]. Hydrotalcite-like compounds (HTlcs) can be applied as adsorbents and ion-exchangers because of their advantages at the aspect of low cost, great adsorption capacity, and their double-layer structure [25,26]. Although some adsorbents [27,28] were investigated to remove nitrate in aqueous solution, the Mg/Fe hydrotalcite's application towards efficient removal of nitrate has not been examined previously. Since both Fe and Mg are common in soil and there is every possibility that a complex compound of Fe–Mg may be present in soil, the present study of adsorption of nitrate on Mg/Fe HTlcs has its significance [29].

The present research was aimed to synthesize, characterize adsorbents, and also to study the removal efficiency of nitrate by Mg/Fe hydrotalcite. The characteristics of adsorbent materials via x-ray diffraction (XRD) and fourier transform infrared spectra (FTIR) were examined to validate the adsorption efficiencies of Mg/Fe hydrotalcite. Various parameters (temperature, adsorbent dose, contact time, pH, initial nitrate concentration, co-existing anions, etc.) during the adsorption of nitrate from aqueous solution were examined. The kinetics and isotherm patterns of adsorption were analyzed to understand the underlying mechanism of nitrate adsorption on Mg/Fe hydrotalcite.

2. Experimental

2.1. Reagents and chemicals

All reagents in this experiment, including $Mg(NO_3)_2{\cdot}6H_2O$, $Fe(NO_3)_3{\cdot}9H_2O$, $Zn(NO_3)_2{\cdot}6H_2O$, $Al(NO_3)_3{\cdot}9H_2O$, NaOH, $NaCO_3$, and KNO_3, were analytical grade. The solutions were all prepared with deionized water. The desired pH was adjusted by adding 0.1 mol/L HNO_3 or 0.1 mol/L NaOH solutions.

2.2. Preparation of Mg/Fe hydrotalcite support

A series of Mg/Fe HTlcs with different Mg/Fe molar rations were synthesized by the co-precipitation method. Two aqueous solutions, A and B, were added simultaneously to a 1 L breaker containing 100 mL of deionized water at room temperature under vigorous stirring. Solution A contained an mixture of $Mg(NO_3)_2{\cdot}6H_2O$ and $Fe(NO_3)_3{\cdot}9H_2O$. Solution B contained NaOH and $NaCO_3$, which was stoichiometric enough to precipitate the salt in the first solution. The pH of the mixed solution was maintained between 9 and 10. The slurry was stirred at 60℃ for 24 h. It was then filtered and washed thoroughly with deionized water till the washings were neutral. The precipitate was dried at 100℃ for 12 h. The calcined hydrotalcites (CHTlcs) were obtained at temperatures 450℃ for 6 h in a muffle furnace. Other CHTlcs containing carbonate as the interlayer anion, such as Mg/Al, Zn/Al, Zn/Fe, and Mg/Al/Fe hydrotalcites, were prepared following the same co-precipitation method.

2.3. Nitrate adsorption experiments

Adsorption of nitrate on CHTlcs was carried out in a batch system. In the flask, 100 mL nitrate solution (100 mg/L) was agitated in a rotary shaker at 250 rpm and ambient temperature (30 ± 2℃). After continuous stirring for 24 h, nitrate concentration was determined by nitrate ion selective electrode and ion analyzer. A number of parameters affecting the adsorption of nitrate ion, such as hydrotalcite composition, adsorbent dose, pH, temperature, contact time, concentration of nitrate, and co-existing anions, were varied widely in order to optimize the removal process. All adsorption trials and sample tests were carried out in triplicates.

2.4. Analytical and characterization methods

Chemical analyses for sulfate, phosphate, chloride, and nitrate in solution were conducted by Dionex ion chromatography (ICS-1000) system. Samples from serum bottles were filtered with a Whatman filter (0.45 um). The IC system was equipped with an EG40 eluent generator, a 1.0 mL sample loop, a set of 4 × 250 mm AS20 and AG 20 columns, a 4 mm ASRS Ultra II suppressor, and a DS3 detection stabilizer.

XRD analysis was performed using a Bruker D8 diffractometer (Germany) with a fitted slit and filtered with a graphite monochromator using Cu-Kα radiation. The samples were step-scanned in steps of 0.02° over the range of 5–90° using a court time of 0.1 s per step at 40 kV and 40 mA.

FTIR was measured by Bruker Vector 33 spectrophotometer (Germany). The samples were recorded in the wave number range from 400 to 4,000 cm^{-1} by using the KBr pellet technique.

3. Results and discussion

3.1. Selection and characterization of adsorbent

CHTlc particles were prepared with various metal cations and were examined for the removal efficiency and the adsorption capacity of nitrate. 0.15 g of CHTlc particles were added to 100 mg/L nitrate solution and were stirred for 24 h. As shown in Fig. 1, Mg/Fe CHTlcs had the highest removal efficiency and adsorption capacity of nitrate which reached to 96.1%, 71.05 mg/g, followed closely by MgAlFe HTlc particles. All other CHTlcs used, exhibited poor nitrate removal efficiency and adsorption capacity. The results found that Mg/Fe CHTlcs was one of the most efficient adsorbents for nitrate removal in the nitrate solution. In the next adsorption process, Mg/Fe CHTlcs was selected for further investigation. In this study, CHTlcs with different Mg/Fe molar ratio were used in adsorption assays to investigate the effect of Mg/Fe molar ratio on nitrate uptake. The result of the study is presented in Fig. 2. The CHTlcs with Mg/Fe ratio of 3 appeared optimal for nitrate adsorption. More Mg^{2+} replacement by Fe^{3+} (e.g. Mg/Fe of 1:1 or 2:1) decreased the percentage removal and the adsorption capacity instead of further improvement. In this study, introduction of more Fe^{3+} would improve the net positive charge of them mixed metal hydroxide layers. On the other hand, too much Fe^{3+} insert may also lead to disorder of the layered hydrotalcite-like structure of HTlc or even phase change due to the radius difference between Mg and Fe, which resulted in the uptake decrease during the nitrate adsorption process [30]. Maximum removal of 97.3% and the adsorption capacity of 72.54 mg/g were obtained by the CHTlcs with 3:1 Mg/Fe molar ratio, followed closely by the CHTlcs with 4:1 and 5:1 Mg/Fe molar ratio. The CHTlc was prepared with 3:1 Mg/Fe molar ratio and was used in the next batch studies.

Nitrogen adsorption isotherm and corresponding pore size distribution of the Mg/Fe CHTlcs are shown in Fig. 3 and the porous structure parameters are compiled in Table 1. According to the classification of IUPAC, the isotherm (Fig. 3(a)) presenting the hysteresis loops between the adsorption and desorption branches can be classified as type-IV, which is characteristic of a mesoporous solid [31]. Moreover, the adsorption isotherm is not present in a plateau at high P/P_0 values, which suggest that N_2 physisorption occur between aggregates of platelet particles and led to the lamellar morphology of the Mg/Fe CHTlcs [31]. The characteristic of mesoporous materials is further

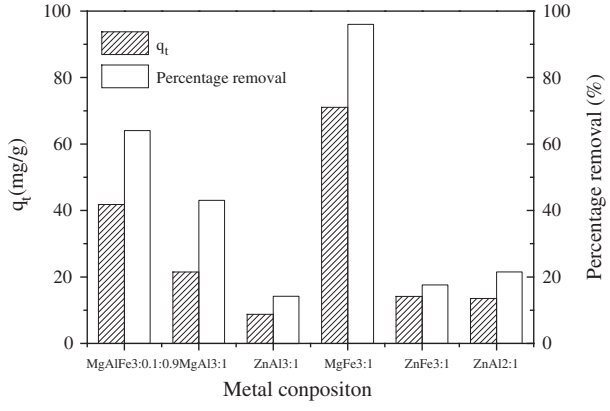

Fig. 1. Effect of metal composition of CHTlcs on nitrate adsorption.

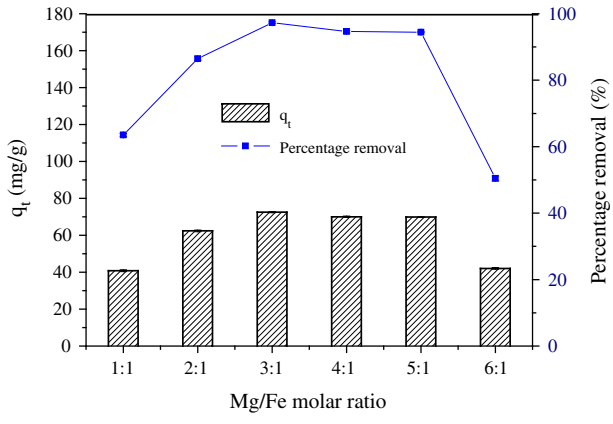

Fig. 2. Effect of Mg/Fe molar ratio on nitrate adsorption.

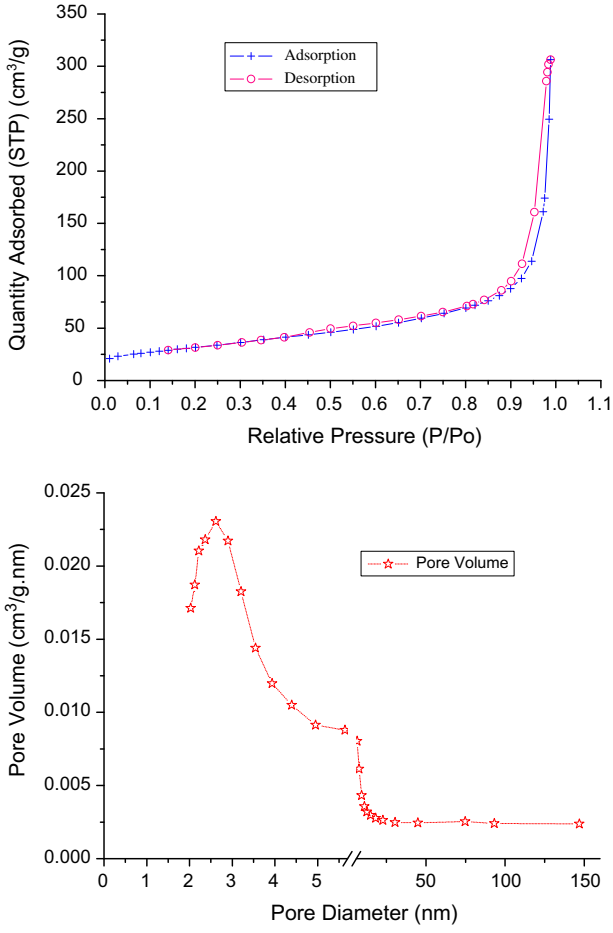

Fig. 3. (a) Isotherm curve of N_2 adsorption–desorption of Mg/Fe CHTlcs. (b) Pore size distribution of Mg/Fe CHTlcs.

confirmed by the pore size distribution in Fig. 3(b). The synthesized Mg/Fe CHTlcs sample has a narrow, unimodal pore size distribution (2–3 nm, maximum at 2.6 nm), and its average pore diameter (8.85 nm) is in the range of mesopores (2–50 nm). This shows mesoporous size is dominated in the adsorbents, which leads to rapid adsorption at the initial adsorbed process. The adsorbed rates become slow for the lack of micropores. The result is consistent with the elaboration in the intraparticle diffusion kinetics model.

3.2. Effect of adsorbent dose

The effect of variation of adsorbent dose on percentage removal and adsorption capacity of nitrate from aqueous solution with CHTlcs used in this study is shown in Fig. 4. The removal efficiency of nitrate increased with increasing dosage of CHTlcs. With the increase in the adsorbent dose from 1.5 to 3.5 g/L at adsorbate concentration of 100 mg/L, the nitrate removal efficiencies exceeded 99.25% and the adsorption capacity of nitrate decreased all the time. From the plot it was observed that 0.15 g CHTlcs was considered as optimum dose during the adsorption process with the initial nitrate concentration of 100 mg/L.

3.3. pH-dependent adsorption study and zeta potential analysis of Mg/Fe CHTlcs

Solution pH is one of the important parameters affecting the adsorption efficiency. The effect of pH on nitrate adsorption was studied in the pH range of 3–11 at an initial nitrate concentration of 100 mg/L and with adsorbent doses of 1.5 g/L. The result is shown in Fig. 5. The adsorption capacity and the percentage removal of nitrate increased as pH was raised from 3 to 8, and reached maximum efficiency at pH about 8 and then decreased as pH increased from 8 to 11. An acidic environment with a pH below 5 adversely affected nitrate uptake due to the significant CHTlcs dissolution as indicated by a sharp increase of Mg^{2+} in bulk water. High concentrations of OH^- ions caused the competitive effect with NO_3^-, which decreased nitrate removal efficiency [32,33]. From the result shown in Fig. 5, it suggested that the optimum pH for removal of nitrate was 8.

As shown in Fig. 6, the zeta potential of Mg/Fe CHTlcs particles is increased from 5.45 to 10.5 mV when pH is changed from 7 to 3. For the Mg/Fe CHTlcs system, the zeta potential reading became

Table 1
Porous structure parameters of the Mg/Fe CHTlcs

S_{BET}[a] (m^2/g)	$S_{ext}/S_{\mu p}$[b] (m^2/g)	V_T[c] (cm^3/g)	$V_{\mu p}$[d] (cm^3/g)	Average pore diameter (nm)
112.7	102.2/10.6	0.249	0.004	8.85

[a]S_{BET}—total surface area.
[b]S_{ext}—external surface area; $S_{\mu p}$—microporous surface area.
[c]V_T—total pore volume.
[d]$V_{\mu p}$—microporous volume.

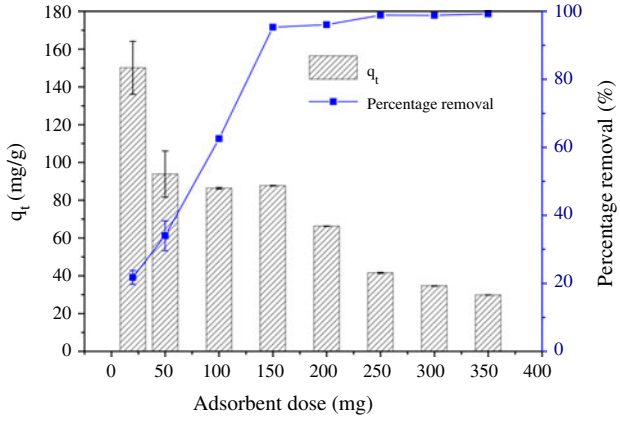

Fig. 4. Effect of adsorbent dose on nitrate adsorption.

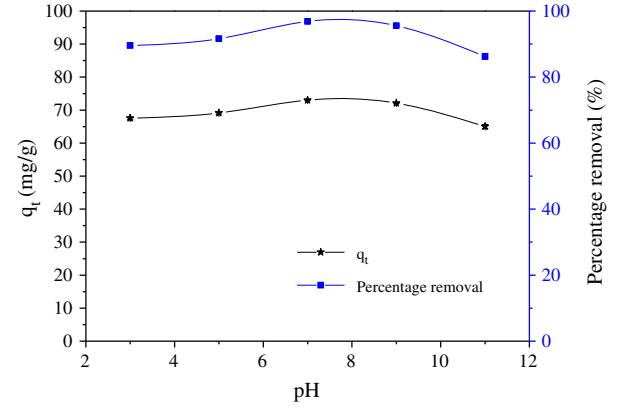

Fig. 5. Effect of pH on nitrate adsorption.

instability when pH was tried to reach below 5, which is probably caused by the dissolution of CHTlcs at pH below 5 [34]. This would lead to the raise of ionic strength in solution, so the zeta potential of CHTlcs was increased. Apart from the effect of the ionic strength, increasing the zeta potential of CHTlcs was presumably caused by Cl^- replacing CO_3^{2-} during the HCl addition. Since the added Cl^- had a less affinity for CHTlcs than CO_3^-, thus the CHTlcs particles shown a higher zeta potential at a lower pH. Moreover, when pH < 7, the surface hydroxide layer started protonation [34]. This would increase the zeta potential of CHTlcs particles. When the solution pH was increased from 7 to 9, the zeta potential of CHTlcs particles was unexpected to be increased. The reason might be that the OH^- ions exchanged with the CO_3^- ions on the CHTlcs. Because OH^- had a less affinity for CHTlcs than CO_3^-, thus the zeta potential of CHTlcs particles was raised at this pH range. However, when pH exceeded 9, the zeta potential of

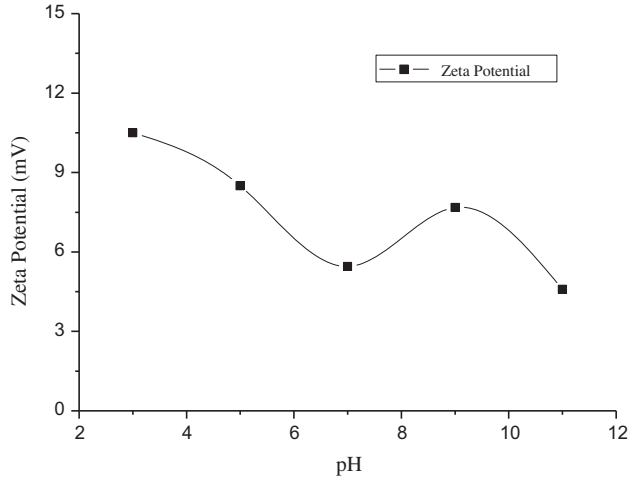

Fig. 6. Plot of the zeta potential of Mg/Fe CHTlcs particle vs. the solution pH.

CHTlcs particles was decreased rapidly. This decrease was mainly due to deprotonation effect. Such a change trend with pH was also reported by Xu et al. for Mg_2Al–CO_3–LDH particles [35].

The zeta potential of CHTlcs was all positively charged in the pH range of 3–11, favoring the adsorption of nitrate. However, when pH < 7, the dissolved load of Mg^{2+} sharply increase with the increase of acidity in the solution [34]. Therefore, the adsorption efficiency of nitrate gradually decrease duo to the increase of the positive charge on the surface of CHTlcs. When pH exceeded 9, the zeta potential of CHTlcs particles was decreased rapidly, causing adverse effect for the adsorption of nitrate. However, when pH was increased from 7 to 9, the zeta potential of CHTlcs particles was increased. So the adsorption efficiency of nitrate was optimal in the pH range of 7–9. These results were agreement with the effect of pH on nitrate adsorption.

3.4. Effect of temperature

The influence of temperature on the adsorption of nitrate with initial concentration 100 mg/L onto 3:1 Mg/Fe CHTlcs was studied in Fig. 7 using optimum adsorbent dose 1.5 g/L. The fraction of nitrate removal as a function of temperature showed that both of the percentage removal and adsorption capacity of nitrate decreased with a rise in the temperature. With the increase of the temperature from 25 to 55 °C, the adsorption capacity of nitrate decreased from 72.45 to 60.57 mg/g, meanwhile the percentage removal of nitrate was dropped down from 93.74 to 78.37%. The increase in the temperature can be

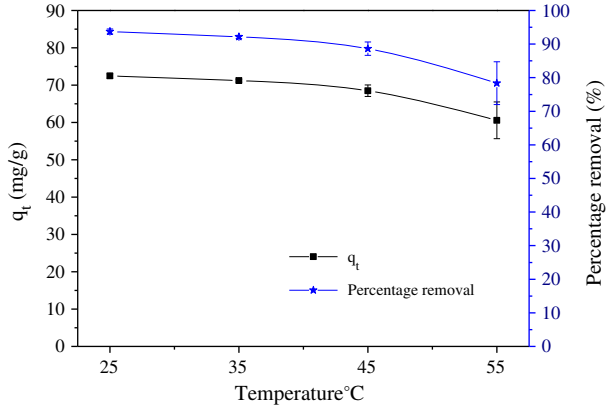

Fig. 7. Effect of temperature on nitrate adsorption.

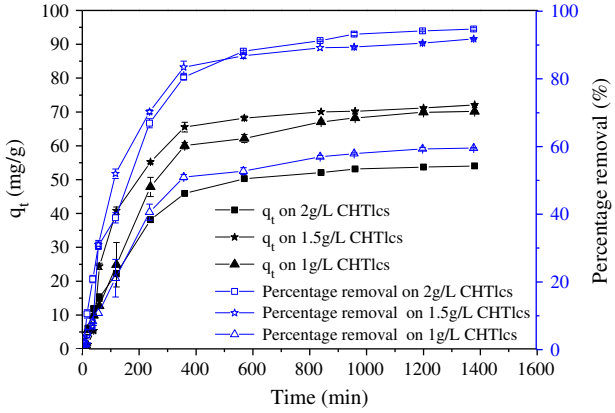

Fig. 8. Effect of contact time on nitrate adsorption with various adsorbent dose.

interpreted as a rise in the kinetic energy of the species in solution, consequently, in an increase of their entropy values. Thus, the higher temperature leads to a decrease of adsorption capacity [36]. Another possible reason is that the adsorption of nitrate is a complex process, whose mechanism may be combination of ion-exchange and physical adsorption [37]. The observation in Fig. 7 indicated that the interaction between adsorbate and adsorbent is exothermic in nature. In order to save the energy and keep the convenience, most of adsorption processes were kept at the room temperature of 30 ± 2℃

3.5. Adsorption kinetic

Most of the adsorption transformation processes are time dependent [38]. Fig. 8 depicts the influence of time on the uptake of nitrate. As illustrated in Fig. 8, the adsorbent capacity and the percentage removal of nitrate increased with the increasing contact time, then reached a maximum at 10 h (optimum time) and thereafter remained almost constant. At the adsorbent dose of 2, 1.5, and 1 g/g, the percentage removal of nitrate was found to increase up to 94.74, 91.79, 59.53%, and the adsorbent capacity increased up to 54.02, 72.09, and 70.13 mg/g, respectively. It can be seen that the 1.5 g/L HTlc had the highest capacity in nitrate (100 mg/L) adsorption, which is in agreement with above-mentioned conclusion obtained from test on effect of adsorbent dose.

To understand the dynamic interactions of nitrate with CHTlcs and to predict their fate with time, four kinetics models, including first-order, pseudo-second-order, Elovich model, and intraparticle diffusion kinetics model, were used to fitting experiment data of nitrate adsorption.

3.5.1. Pseudo-first-order model

This model was suggested by Lagergren [39] for the sorption of solid/liquid systems, which based on the assumption of proportionality between the adsorption rate and the number of free adsorption sites. The differential equation is generally expressed as:

$$\frac{dq_t}{dt} = k_1 (q_e - q_t) \tag{1}$$

Integrating the above equation by considering the following boundary condition, $q_t = 0$ at $t = 0$, Eq. (1) becomes:

$$\ln (q_e - q_t) = \ln (q_e) - k_1 t \tag{2}$$

where q_e and q_t represent the amounts of nitrate adsorbed onto the adsorbents at equilibrium and at time t, respectively (mg/g), and k_1 is the rate constant of pseudo-first-order adsorption (min^{-1}). The plot of $\ln (q_e - q_t)$ vs. t (present in Fig. 9(a)) gives a straight line for the pseudo-first-order adsorption kinetics, which allows the values of q_e and k_1 to be computed. The k_1 values, the correlation coefficients, R^2, and q_e values are listed in Table 2. The regression coefficient values determined were 0.953, 0.823, and 0.978 for 1.0, 1.5, and 2.0 g/L CHTlcs, respectively. The linearity alone did not establish a first-order mechanism.

3.5.2. Pseudo-second-order

This model was supposed that chemical adsorption was the rate-limiting step. It can be shown:

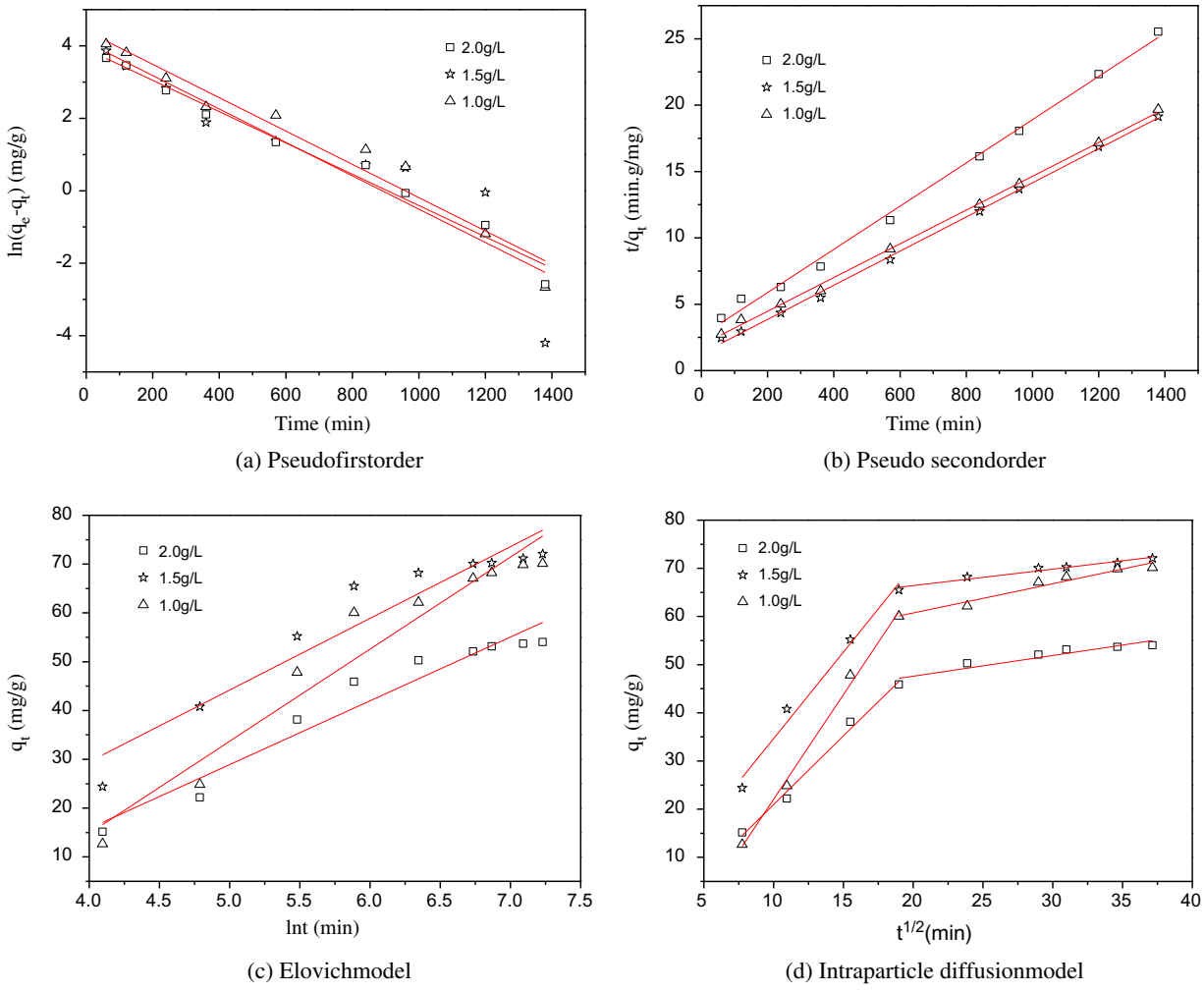

(a) Pseudofirstorder (b) Pseudo secondorder

(c) Elovichmodel (d) Intraparticle diffusionmodel

Fig. 9. Predicted curves by the kinetic analysis of the pseudo-first, pseudo-second-order, Elovich and intraparticle diffusion models at different dose of adsorbents.

$$\frac{dq_e}{dt} = k_2 (q_e - q_t)^2 \tag{3}$$

The equation can be rearranged as follow:

$$\frac{t}{q_t} = \frac{1}{k_2 q_e^2} + \frac{t}{q_e} \tag{4}$$

where k_2 is the second-order rate constant. Linear lines obtained from the variation of t/qt against t according to pseudo-second-order model, which was illustrated in Fig. 9(b). q_e and k_2 rate constants from the slope and intercept have been calculated and listed in Table 2. The experimental data showed a good fitting with the pseudo-second-order model and the correlation coefficients for the linear plots were higher than 0.994.

3.5.3. Elovich model

The Elovich equation is satisfied in chemical adsorption processes, and is suitable for systems with heterogeneous adsorbing surfaces. The rate expression for the adsorption is described:

$$\frac{dq_t}{dt} = \alpha \exp(-\beta q_t) \tag{5}$$

Given that $q_t = q_t$ at $t = t$ and $q_t = 0$ at $t = 0$, the Eq. (5) can be simplified as:

$$q_t = \beta \ln(\alpha\beta) + \beta \ln(t) \tag{6}$$

where both α and β are constants during the adsorption process, which are listed in Table 2. The predicted curves of Elovich model was depicted in Fig. 9(c). The

Table 2
Kinetic parameters obtained by fitting experimental data to the pseudo-first-order, pseudo-second-order, Elovich and intraparticle diffusion model

Model	Parameter	CHTlcs (1.0 g/L)	CHTlcs (1.5 g/L)	CHTlcs (2.0 g/L)
Pseudo first order	q_e	82.17	60.29	49.91
	$K_1 \times 10^{-3}$	4.60	4.61	4.32
	R^2	0.953	0.823	0.978
Pseudo second order	q_e	78.62	77.70	61.39
	$K_2 \times 10^{-5}$	8.42	12.91	10.13
	R^2	0.994	0.998	0.996
Elovich model	α	0.002126	0.009246	0.004694
	β	18.88	14.71	13.08
	R^2	0.933	0.906	0.937
Intraparticle diffusion model	k_{ip1}	4.34	3.59	2.85
	R_1^2	0.993	0.977	0.987
	k_{ip2}	0.61	0.34	0.43
	R_2^2	0.951	0.959	0.878

correlation coefficients for this model were ranged from 0.906 to 0.937, which indicated that the adsorption data was not fit for the Elovich model very well.

3.5.4. Intraparticle diffusion kinetics model

In order to test the importance of internal mass transfer in the adsorption process, kinetic data were used further to check the possibility of intraparticle diffusion by using the Weber and Morris equation. Its linear form is:

$$q_t = k_{ip} t^{1/2} + C \tag{7}$$

where k_{ip} is the intraparticle diffusion rate, and C is a constant. As shown in Fig. 9(d), the plot of qt vs. $t^{1/2}$ was multilinear, which indicated two or more stages influence the adsorption process [40]. The first line could be attributed to adsorption of the nitrate over the shell and macropore of adsorbents, and the second line was ascribed to the intraparticle diffusion through micropores.

3.5.5. Kinetic model analysis

Fig. 9 depicts the four kinetic models plots for the adsorption of nitrate onto Mg/Fe CHTlcs, respectively. Various parameters from these kinetic models are summarized in Table 2. From the correlation coefficient, R^2, of these four kinetic models, it was observed that kinetic data were fit to the pseudo-second-order kinetic model best. Also, the calculated q_e values from pseudo-second-order kinetic model agreed well with the experimental data. The equilibrium adsorption capacities increased with an increase in adsorbent dose. The good agreement of the data with the pseudo-second-order kinetics model suggested that the chemisorptions process could be a rate-limiting step.

3.6. Isotherm

Adsorption equilibrium is usually described by isotherm equation which expresses the relationship between nitrate concentration in solution and the amount of nitrate adsorbed on a specific adsorbent at a fixed pH and temperature [41]. The experiments were performed at usual temperature (30 ± 2°C) to discuss the effect of initial nitrate concentration on nitrate adsorption. The equilibrium isotherm of nitrate uptake by Mg/Fe CHTlcs from synthetic water is shown in Fig. 10. Isotherms for nitrate sorption by Mg/Fe CHTlcs were modeled by two commonly used isotherm equations: Langmuir and Freundlich. The adsorption constants of isotherms are listed in Table 3.

The Freundlich isotherms model is expressed by the equation:

$$q_e = k_f \times C_e^{1/n} \tag{8}$$

The above equation can be rearranged in its logarithmic form:

$$\ln q_e = \ln k_f + \frac{1}{n} \ln C_e \tag{9}$$

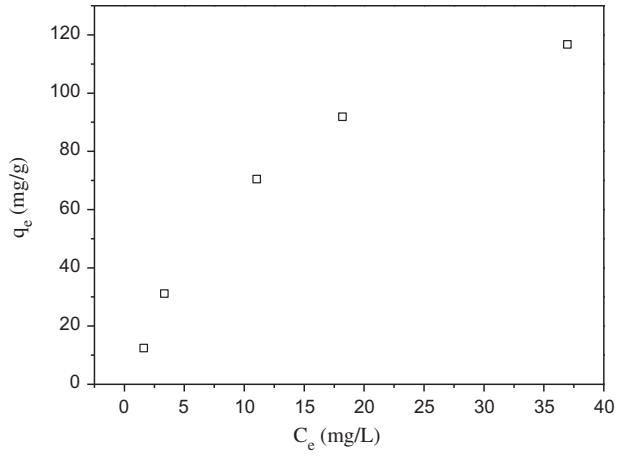

Fig. 10. Plot of equilibrium sorption capacity vs. equilibrium concentration for nitrate.

where q_e is the amounts of nitrate adsorbed at equilibrium (mg/g), C_e is the aqueous concentration of nitrate in solution at equilibrium (mg/L), k_f is the Freundlich constant, and n is the adsorption intensity.

The Langmuir isotherm model is valid for monolayer adsorption onto surface containing finite number of identical sorption sites which is presented by following Eq. (10):

$$q_e = \frac{q_m k_L C_e}{1 + k_L C_e} \tag{10}$$

This model can be arranged in its linear form:

$$\frac{C_e}{q_e} = \frac{1}{bq_m} + \frac{C_e}{q_m} \tag{11}$$

where q_e is the equilibrium adsorption concentration of nitrate by adsorbent (mg/g), C_e is the nitrate concentration in the equilibrium solution (mg/L), b is the Langmuir constant related to the adsorption energy, and q_m is the saturated adsorption capacity (mg/g).

In order to analyze the adsorption efficiency for the Langmuir model, a dimensionless constant is investigated as follow:

$$R_L = \frac{1}{1 + bC_0} \tag{12}$$

where R_L is the equilibrium parameter, C_0 is the initial concentration of nitrate.

It can be seen from Table 3 that the Langmuir isotherm is a better fit to the experimental data than the Freundlich isotherm on the basis of the correlation coefficients (R^2). Many researchers [20,42,43] agreed that Langmuir isotherm was a good model to fit for oxyanion adsorption on CHTlcs. Value of $R_L < 1$ represents favorable adsorption. The R_L-value for the adsorption process with initial nitrate concentration of 100 mg/L was found to be 0.129, which indicated a favorable adsorption system.

3.7. Effect of competitive ions

Due to various anions, such as sulfate, phosphate, chloride, and nitrate, coexisting in reality water system, it is necessary to investigate effect of interfering ions during the adsorption of nitrate. The effect of these competitive anions on adsorption was investigated by determining the amount of the nitrate adsorption at different concentrations of Cl^-, SO_4^{2-}, PO_4^{3-} ranging from 50 to 200 mg/L at pH 8 with the initial nitrate concentration of 100 mg/L. The systems of $Cl^- + NO_3^-$, $SO_4^{2-} + NO_3^-$, $PO_4^{3-} + NO_3^-$ were tested with results shown in Fig. 11. It was clear from Fig. 11 that presence of these anions reduced the nitrate adsorption. The inhibitory effect was in the order of phosphate > sulfate > chloride. The effect of these anions towards adsorption may be due to their affinity towards Mg/Fe oxide. Again, layered double hydroxides have greater affinities for anions with higher charge density, i.e. the tendency of multicharge anions to get adsorbed are more than that of monovalent anions.

3.8. Characterization contrast samples before and after adsorption

As a direct means for giving information about surface and bulk species [32], FTIR study of Mg/Fe

Table 3
Freundlich and Langmuir constants for nitrate adsorption on CTHlcs

			Freundlich				Langmuir		
C_0 mg/L	CHTlcs g/L	T°C	n	K_f	R^2	q_m	b_L	R_L	R^2
100	1.5	25	1.410	10.968	0.940	163.934	0.0678	0.129	0.998

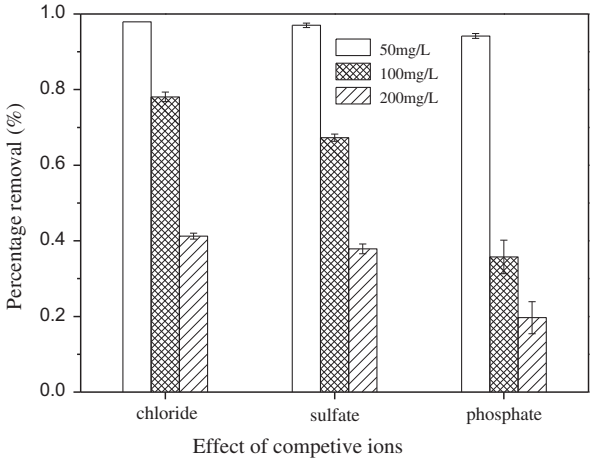

Fig. 11. Nitrate removal by CHTlcs with co-existing anions.

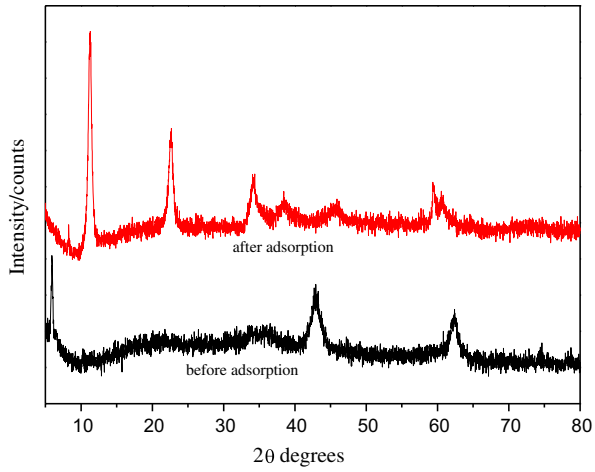

Fig. 13. X-ray patterns of CHTlcs.

CHTlcs was carried out to investigate the presence of different groups, structures and adsorption of nitrate onto CHTlcs. The results were presented in Fig. 12. The broad band at around 3,500 cm^{-1} indicated the presence of OH^- groups in hydrogen bond stretching in the interlayer OH^- groups. The small adsorption peaks in the region 1,650–1,600 cm^{-1} are attributed to bending mode of water molecules and interlamellar carbonate ions [25]. After adsorption of nitrate, the band observed at around 1,400 cm^{-1} become very strong and sharp and shifted to higher wavenumber (Fig. 12(b)). This could be due to the reconstruction of the oxide material in the presence of nitrate, which was characteristic of CHTlcs [44]. The bands between 500 and 700 cm^{-1} could be attributed to the superposition of the characteristic vibrations of magnesium and ferric oxides [30].

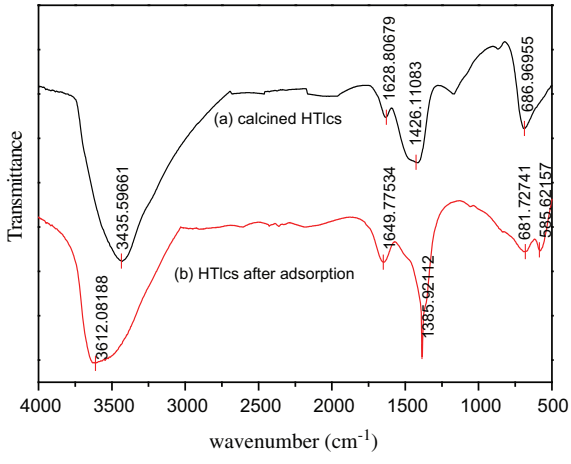

Fig. 12. FTIR spectra of CHTlcs.

The XRD analysis was used to identify the composition structures, which was shown in Fig. 13. After calcination, the peaks corresponding to (003) and (006) planes disappeared, indicating that hydrotalcite structure was changed. When the sample was mixed in nitrate aqueous solution, the XRD pattern showed regeneration of hydrotalcite phase [45]. Anion incorporation was occurred simultaneously during the adsorption process, which was helpful to increase the anionic exchange capacity of CHTlcs [40].

4. Conclusions

Mg/Fe CHTlcs was successfully applied to remove nitrate from water in batch experiments. This CHTlcs with 3:1 Mg/Fe molar ratio presented high efficiency in nitrate adsorption, and the maximum adsorption capacity was about 70 mg/g. The effective range of pH for nitrate removal was between 5.0 and 8.0. The lower adsorption capacity in CHTlcs with the increased temperature indicated the exothermic nature of nitrate adsorption in CHTlcs. The anions of higher valence had a more significant interfering effect than the monovalent anions in the nitrate adsorption by CHTlcs. The adsorption of nitrate on the used Mg/Fe CHTlcs could be well-described by pseudo-second-order kinetics and the data agreed well with the Langmuir isotherm model. The results deriving from this study suggested that the Mg/Fe CHTlcs is a promising adsorbent for the removal of nitrate for water remediation because of its high adsorption capacity and low cost.

Acknowledgements

The research has been funded by the project of National Natural Science Foundation of China (NSFC) (51008128, 41071305), the Fundamental Research Funds for the Central Universities (2011ZM0052).

References

[1] M.H. Ward, T.M. deKok, P. Levallois, J. Brender, G. Gulis, B.T. Nolan, J. VanDerslice, Workgroup report: drinking-water nitrate and health—Recent Findings and Research Needs, Environ. Health Perspect. 113 (2005) 1607–1614.
[2] N. Barrabés, M.A. Garrido, A. Frare, A. Monzón, D. Tichit, Pt-MgZnCuAl hydrotalcite-derived catalysts in the reduction of nitrates using continuous and batch reactors, Catal. Today 175 (2011) 328–337.
[3] N. Öztürk, T.E. Bektas, Nitrate removal from aqueous solution by adsorption onto various materials, J. Hazard. Mater. 112 (2004) 155–162.
[4] D. Majumdar, N. Gupta, Nitrate pollution of groundwater and associated human health disorders, Indian J. Environ. Health 42 (2000) 28–39.
[5] S.H. Lin, C.L. Wu, Removal of nitrogenous compounds from aqueous solution by ozonation and ion exchange, Water Res. 30 (1996) 1851–1857.
[6] K. Mizuta, T. Matsumoto, Y. Hatate, K. Nishihara, T. Nakanishi, Removal of nitrate-nitrogen from drinking water using bamboo powder charcoal, Bioresour. Technol. 95 (2004) 255–257.
[7] K. Kimura, M. Nakamura, Y. Watanabe, Nitrate removal by a combination of elemental sulfur-based denitrification and membrane filtration, Water Res. 36 (2002) 1758–1766.
[8] M.I.M. Soares, Biological denitrification of groundwater, Water Air Soil Pollut. 123 (2000) 183–193.
[9] A. Nuhoglu, T. Pekdemir, E. Yildiz, B. Keskinler, G. Akay, Drinking water denitrification by a membrane bio-reactor, Water Res. 36 (2002) 1155–1166.
[10] A.E. Palomares, J.G. Prato, F. Márquez, A. Corma, Denitrification of natural water on supported Pd/Cu catalysts, Appl. Catal., B 41 (2003) 3–13.
[11] Y. Wang, J. Qu, H. Liu, Effect of liquid property on adsorption and catalytic reduction of nitrate over hydrotalcite-supported Pd-Cu catalyst, J. Mol. Catal. A: Chem. 272 (2007) 31–37.
[12] A. Santafé-Moros, J.M. Gozálvez-Zafrilla, J. Lora-García, Performance of commercial nanofiltration membranes in the removal of nitrate ions, Desalination 185 (2005) 281–287.
[13] A. Bhatnagar, M. Sillanpää, A review of emerging adsorbents for nitrate removal from water, Chem. Eng. J. 168 (2011) 493–504.
[14] M. Dore, Ph. Simon, A. Deguin, J. Victot, Removal of nitrate in drinking water by ion exchange-impact on the chemical quality of treated water, Water Res. 20 (1986) 221–232.
[15] S. Samatya, N. Kabay, Ü. Yüksel, M. Arda, M. Yüksel, Removal of nitrate from aqueous solution by nitrate selective ion exchange resins, React. Funct. Polym. 66 (2006) 1206–1214.
[16] J.J. Schoeman, A. Steyn, Nitrate removal with reverse osmosis in a rural area in South Africa, Desalination 155 (2003) 15–26.
[17] D. Wan, H. Liu, X. Zhao, J. Qu, S. Xiao, Y. Hou, Role of the Mg/Al atomic ratio in hydrotalcite-supported Pd/Sn catalysts for nitrate adsorption and hydrogenation reduction, J. Colloid Interface Sci. 332 (2009) 151–157.
[18] S.J.T. Pollard, G.D. Fowler, C.J. Sollars, R. Perry, Low-cost adsorbents for waste and wastewater treatment: A review, Sci. Total Environ. 116 (1992) 31–52.
[19] A. Bhatnagar, M. Sillanpää, Utilization of agro-industrial and municipal waste materials as potential adsorbents for water treatment—A review, Chem. Eng. J. 157 (2010) 277–296.
[20] T. Wu, D. Sun, Y. Li, H. Zhang, F. Lu, Thiocyanate removal from aqueous solution by a synthetic hydrotalcite sol, J. Colloid Interface Sci. 355 (2011) 198–203.
[21] C. Namasivayam, D. Sangeetha, Kinetic studies of adsorption of thiocyanate onto $ZnCl_2$ activated carbon from coir pith, an agricultural solid waste, Chemosphere 60 (2005) 1616–1623.
[22] C. Namasivayam, M.V. Sureshkumar, Modelling thiocyanate adsorption onto surfactant-modified coir pith, an agricultural solid 'waste', Process Saf. Environ. Prot. 85 (2007) 521–525.
[23] Z. Yang, O. Xiao, B. Chen, L. Zhang, H. Zhang, X. Niu, S. Zhou, Perchlorate adsorption from aqueous solution on inorganic-pillared bentonites, Chem. Eng. J. 223 (2013) 31–39.
[24] L.M. Camacho, A. Torres, D. Saha, S. Deng, Adsorption equilibrium and kinetics of fluoride on sol–gel-derived activated alumina adsorbents, J. Colloid Interface Sci. 349 (2010) 307–313.
[25] T. Wang, Z. Cheng, B. Wang, W. Ma, The influence of vanadate in calcined Mg/Al hydrotalcite synthesis on adsorption of vanadium (V) from aqueous solution, Chem. Eng. J. 181–182 (2012) 182–188.
[26] S. Mandal, S. Mayadevi, Adsorption of fluoride ions by Zn–Al layered double hydroxides, Appl. Clay Sci. 40 (2008) 54–62.
[27] J. Olanrewaju, B.L. Newalkar, C. Mancino, S. Komarneni, Simplified synthesis of nitrate form of layered double hydroxide, Mater. Lett. 45 (2000) 307–310.
[28] M.D. Ureña-Amate, N.D. Boutarbouch, M.M. Socias-Viciana, E. González-Pradas, Controlled release of nitrate from hydrotalcite modified formulations, Appl. Clay Sci. 52 (2011) 368–373.
[29] J. Das, D. Das, G.P. Dash, K.M. Parida, Studies on Mg/Fe hydrotalcite-like-compound (HTlc): removal of inorganic selenite (SeO_3^{2-}) from aqueous medium, J. Colloid Interface Sci. 251 (2002) 26–32.
[30] M. Islam, R. Patel, Nitrate sorption by thermally activated Mg/Al chloride hydrotalcite-like compound, J. Hazard. Mater. 169 (2009) 524–531.
[31] Y. Guo, Z. Zhu, Y. Qiu, J. Zhao, Synthesis of mesoporous Cu/Mg/Fe layered double hydroxide and its adsorption performance for arsenate in aqueous solutions, J. Environ. Sci. 25 (2013) 944–953.
[32] J. Das, D. Das, K. Parida, K.M. Parida, Physicochemical characterization and adsorption behavior of calcined Zn/Al hydrotalcite-like compound (HTlc) towards removal of fluoride from aqueous solution, J. Colloid Interface Sci. 261 (2003) 213–220.

[33] M. Islam, R. Patel, Physicochemical characterization and adsorption behavior of Ca/Al chloride hydrotalcite-like compound towards removal of nitrate, J. Hazard. Mater. 190 (2011) 659–668.
[34] K.M. Tyner, S.R. Schiffman, E.P. Giannelis, Nanobiohybrids as delivery vehicles for camptothecin, J. Control. Release 95 (2004) 501–514.
[35] Z. Xu, Y. Jin, S. Liu, Z. Hao, G. Lu, Surface charging of layered double hydroxides during dynamic interactions of anions at the interfaces, J. Colloid Interface Sci. 326 (2008) 522–529.
[36] D.R.M. José, S. Fabiano, T. Jairo, B.V. Joao, Effects of pH, temperature, and ionic strength on adsorption of sodium dodecylbenzenesulfonate into Mg-Al-CO_3 layered double hydroxides, J. Phys. Chem. Solids 65 (2004) 487–492.
[37] L. Kentjono, J.C. Liu, W.C. Chang, C. Irawan, Removal of boron and iodine from optoelectronic wastewater using Mg–Al (NO_3) layered double hydroxide, Desalination 262 (2010) 280–283.
[38] R. Katal, M.S. Baei, H.T. Rahmati, H. Esfandian, Kinetic, isotherm and thermodynamic study of nitrate adsorption from aqueous solution using modified rice husk, J. Ind. Eng. Chem. 18 (2012) 295–302.
[39] S. Gammoudi, N. Frini-Srasra, E. Srasra, Influence of exchangeable cation of smectite on HDTMA adsorption: Equilibrium, kinetic and thermodynamic studies, Appl. Clay Sci. 69 (2012) 99–107.
[40] C. Long, A. Li, H. Wu, Q. Zhang, Adsorption of naphthalene onto macroporous and hypercrosslinked polymeric adsorbent: Effect of pore structure of adsorbents on thermodynamic and kinetic properties, Colloids Surf., A 333 (2009) 150–155.
[41] S. Sohn, D. Kim, Modification of Langmuir isotherm in solution systems—Definition and utilization of concentration dependent factor, Chemosphere 58 (2005) 115–123.
[42] M. Bouraada, M. Lafjah, M.S. Ouali, L.C. de Menorval, Basic dye removal from aqueous solutions by dodecylsulfate- and dodecyl benzene sulfonate-intercalated hydrotalcite, J. Hazard. Mater. 153 (2008) 911–918.
[43] W. Ma, N. Zhao, G. Yang, L. Tian, R. Wang, Removal of fluoride ions from aqueous solution by the calcination product of Mg–Al–Fe hydrotalcite-like compound, Desalination 268 (2011) 20–26.
[44] F. Cavani, F. Trifirò, A. Vaccari, Hydrotalcite-type anionic clays: Preparation, properties and applications, Catal. Today 11 (1991) 173–301.
[45] Y. Wang, J. Qu, H. Liu, C. Hu, Adsorption and reduction of nitrate in water on hydrotalcite-supported Pd-Cu catalyst, Catal. Today 126 (2007) 476–482.